Supplementary Information

A water-stable, light-weight, MOF-based membrane for mitigating polysulfides shuttling in Li-S batteries

Juan Xu, Zheng Lin, Yuan Lei, Xingrun Huang, Chao Chen*

School of Chemical Engineering and Light Industry, Guangdong University of Technology, Guangzhou 510006, China.

E-mail: c.chen@gdut.edu.cn

Experimental section

Synthesis of PLMOF(Co)

PLMOF(Co) was prepared via a conventional hydrothermal method [1]. Typically, 1.5 mmol $Co(NO_3)_2 \cdot 6H_2O$ was dissolved in 5 mL deionized water by stirring to form the solution A. 1.5 mmol NaOH, 1 mmol 4, 5-imidazole dicarboxylic acid and 1 mmol 4, 4′ -bipyridine were added into 5 mL deionized water with stirring to form the solution B. Solution A and B were mixed to form a mixture, which was transferred into a 25 mL teflon-lined autoclave and kept statically under autogenous pressure at 180 °C for 72 hours. The resultant solid were washed with H_2O and finally dried to obtain the PLMOF (Co) product.

Fabrication of the PLMOF (Co)@G-coated *separator*

In a typical procedure, 5.4 mg of PLMOF (Co), 12.6 mg of graphene, and 2 mg of PVDF was dispersed in NMP by sonication for 1 hour to form a uniform black suspension.

Specific amount of the above suspension was then deposited onto a Celgard 2400 separator by a vacuum filter. The loading amount of PLMOF (Co)@G on the PP separator was controlled to be 0.32 mg cm^{-2}, 0.16 mg cm^{-2}, and 0.08 mg cm^{-2}, respectively.

Visualized polysulfide adsorption and permeation tests

Li_2S_6 solution (0.2 M) was firstly prepared by mixing sublimed sulfur and Li_2S in DOL/DME solution (1:1 in vol), which was stirred at 70 °C for 12 h in the glovebox. For the adsorption test, the Li_2S_6 solution was diluted to 2 mM. 50 mg PLMOF (Co) was added to 6 mL Li_2S_6 solution for 7 h. For the diffusion test, the Li_2S_6 solution was diluted to 10 mM. The permeation process of polysulfides through the PP separator and the PLMOF (Co) @G-modified separator was tested using an H-type cell filled with dark brown Li_2S_6 solution (left) and pellucid DOL/DME solution (right).

Cells assembly and electrochemical measurements

S/CNT composite (S: CNT = 8:2 in mass) was firstly prepared using a melting diffusion method. Then the S/CNT composite, CNT and PVDF were mixed at a mass ratio of 7:2:1 in NMP to obtain the cathode slurry, which was coated on an aluminum foil, dried at 60 °C under vacuum, and cut into a 14 mm diameter plate. The average sulfur loading on the cathode was controlled to be 1.0 mg cm^{-2}. The electrolyte is consist of 1 M LiTFSI in DOL/DME (1 : 1 in v/v) with 1% $LiNO_3$ as an additive, and the electrolyte dosage was 15 μL mg^{-1} S. The galvanostatic charge/discharge (GCD) and cycle performance were measured using a LAND battery system in the range of 1.7–2.8 V. The cyclic voltammetry (CV) and electroelectrochemical impedance spectrascopy (EIS) were performed on a CHI 650E electrochemical station. The voltage test window for the CV curve is 1.7 to 2.8 V

with a scan rate of 0.1 mV s^{-1}. EIS was performed over the scanning frequency range of 0.01 Hz-100 kHz.

Material characterization

XRD patterns were recorded using a Rigaku-mini Flex600 X-ray diffractomete (Cu Kα λ=1.54059 Å). The content of S was determined by a thermogravimetric analyzer (NETZSCH TG 209 F3) under argon atmosphere with a heating rate of 5 ^{o}C min^{-1}. X-ray photoelectron spectroscopy (XPS) was performed on an Escalab 250Xi (Thermo Fisher) with Al Kα radiation under argon atmosphere. Textural properties of samples were obtained by N_2 adsorption-desorption measurement carried out on the Belsorp-mini (II) under liquid nitrogen temperature (-196 ^{o}C). Morphologies of samples were characterized by a field-emission scanning electron microscope (FE-SEM, ZEISS sigma500) at 15 Kv and transmission electron microscope (TEM, JEOL JEM-2100 F) with energy dispersive X-ray spectroscopy (EDS). The content of metal atom was determined by the Agilent 725 inductively coupled plasma optical emission spectrometer (ICP). The UV-Vis absorption spectra were obtained using a Persee TU-1900 spectrophotometer.

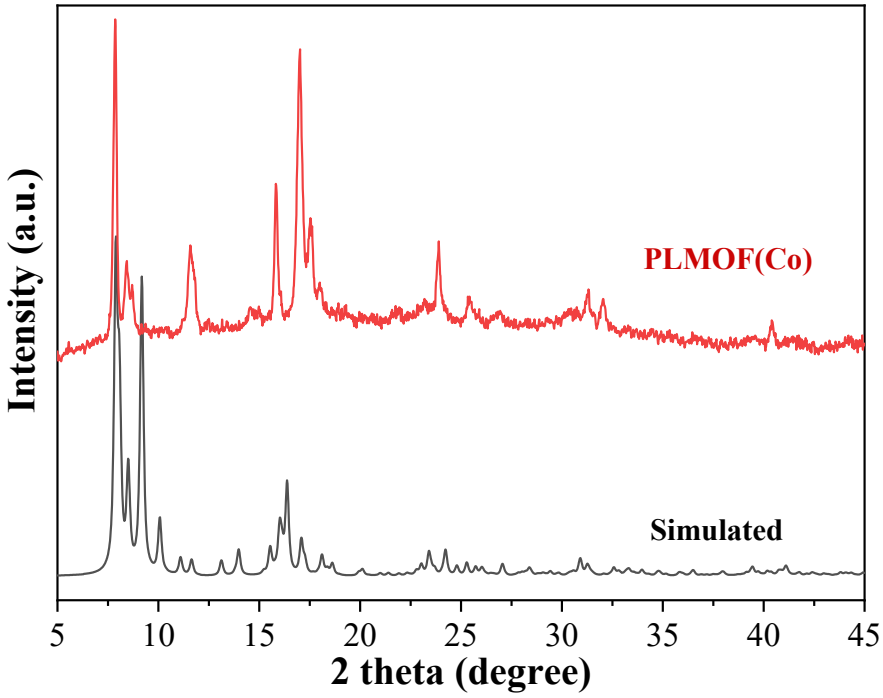

Fig. S1 XRD pattern of the PLMOF(Co).

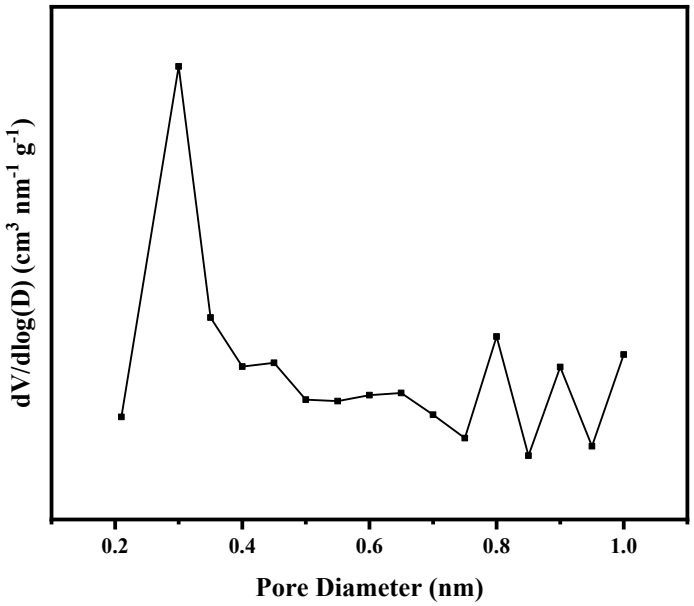

Fig. S2 Micropore size distribution curve of the PLMOF(Co) based on the MP-plot.

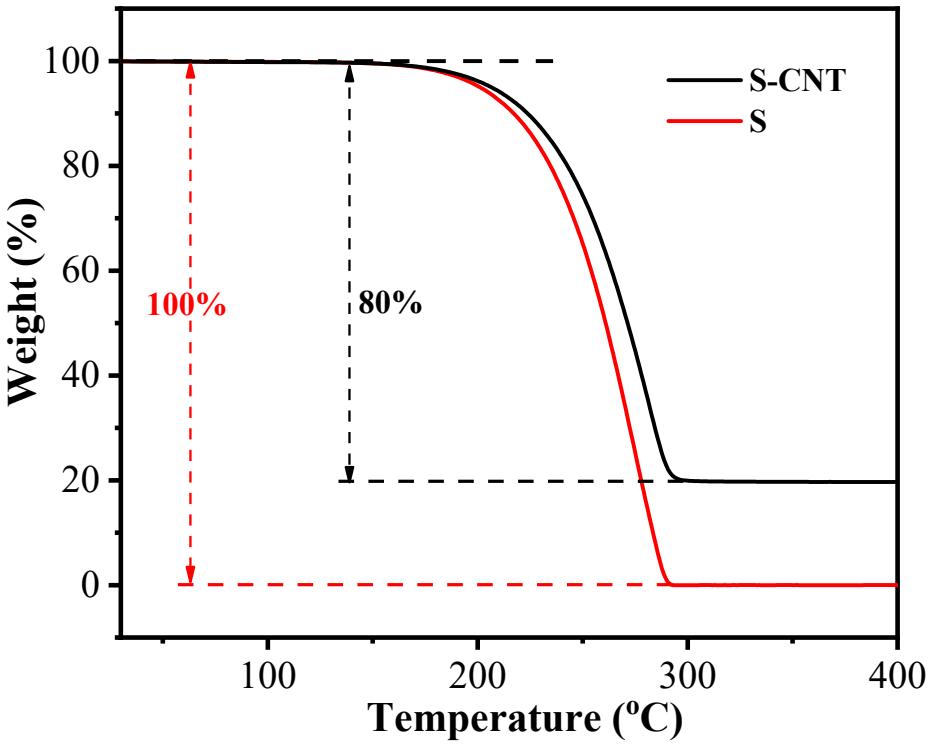

Fig. S3 TGA curves of sulfur and the S/CNT composite.

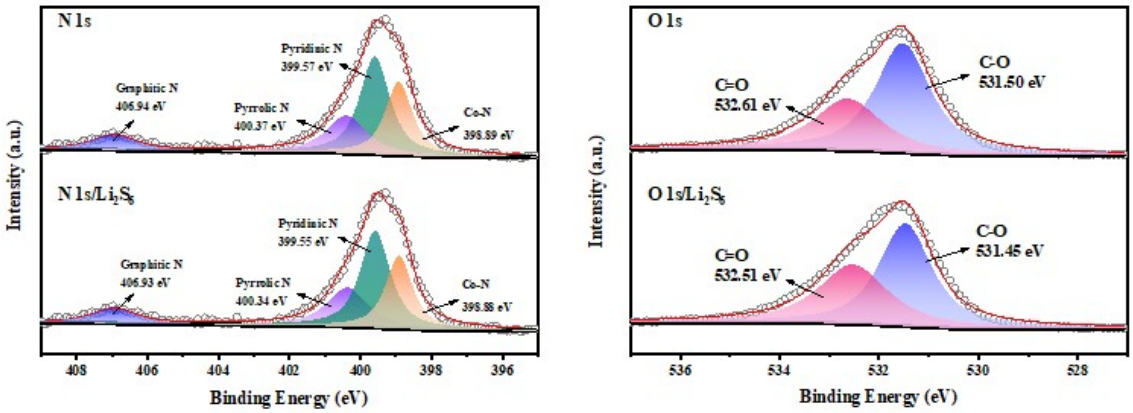

Fig. S4 High-resolution N1s and O1s XPS spectra of the PLMOF(Co) before and after Li_2S_6 adsorption

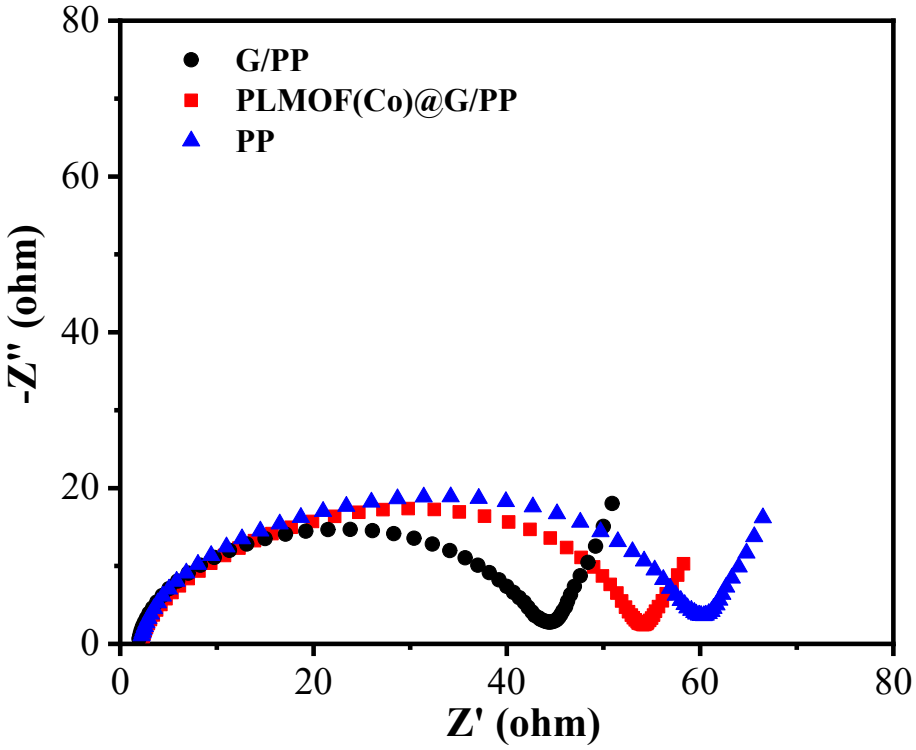

Fig. S5 Nyquist plots of cells assembled with different separators.

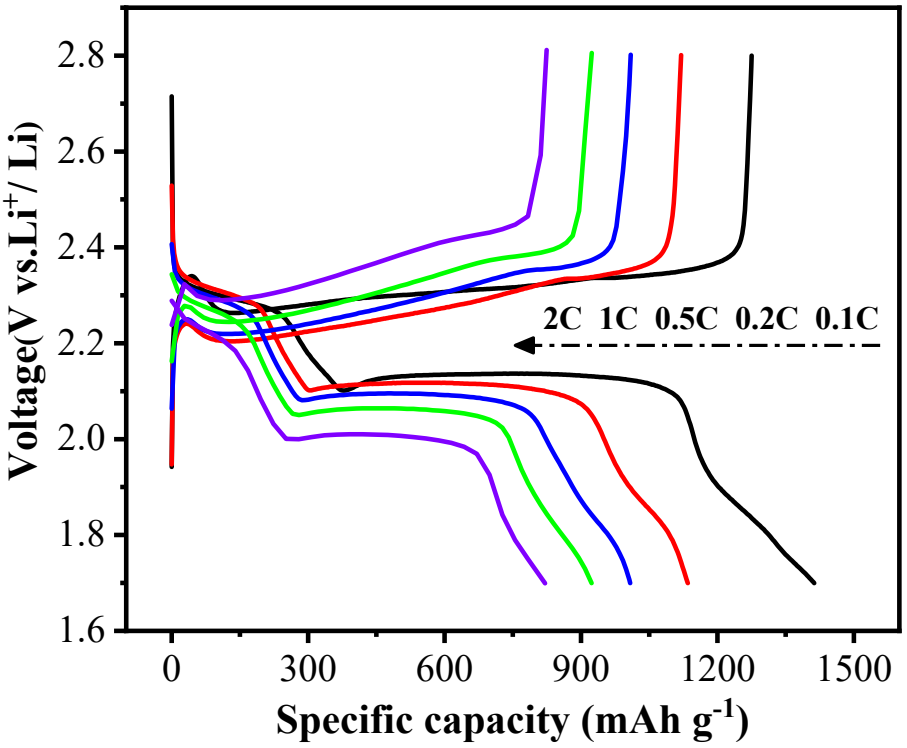

Fig. S6 Galvanostatic discharge-charge profile of the cell assembled with the PLMOF(Co)@G-modified separator.

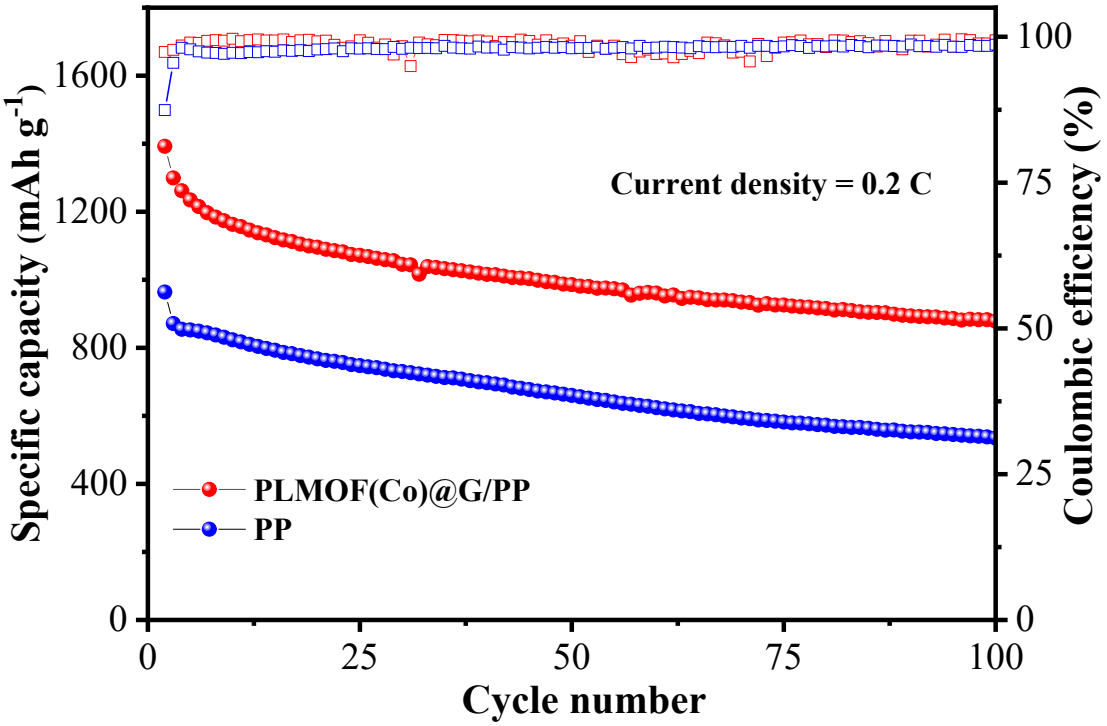

Fig. S7 A comparison of cycle performances of cells assembled with PP and PLMOF(Co)@G-modified separator.

Table S1. A comparison of Li-S battery performance based on the PLMOF(Co)@G-modified separator in this work with other previously reported works.

Interlayer Materials	Cathode	C Rate	1st Capacity (mAh g^{-1})	Cycle	Capacity retention (mAh g^{-1})	Ref.
Y-FTZB	S/Super P	0.25	987	100	～650	[2] ACS Energy Lett.
$Ni_3(HITP)_2$	S/CNT	0.5	990	200	905	[3] Adv. Energy Mater.
B/2D MOF-Co	S/C	0.5	801	200	703	[4] Adv. Mater.
CNT@ZIF-30	S/AB	0.2	1588	100	870	[5] Energy Stor. Mater.
PSS@HKUST-1	S/Super P	0.5	1243	100	968	[6] ACS Appl. Mater. Inter.
$Ni_3(HITP)_2$	S/Super P	0.5	-	100	～740	[7] ACS Appl. Mater. Inter.
UiO-66-NH_2	S/SG	0.1	-	100	560	[8] J. Mater. Chem. A
VN	S/CNT	0.5	1050	100	860	[9] ACS Appl. Mater. Inter.
Cr_3C_2	S/KB	0.5	865	100	～795	[10] Ind. Eng. Chem. Res.
Co_3Mo_3C	S/Super P	0.1	1251	100	905	[11] Sci. China Mater.
Ni-Co-P@C	S/CNTs	0.5	1000	100	～700	[12]

						Energy Stor. Mater.
FMSiNP	**S/KB**	**1**	**1080**	**400**	**660**	**[13]** **J. Mater. Chem. A**
MWCNT/NCQD	**S/KB**	**2**	**953**	**300**	**600**	**[14]** **Adv. Energy Mater.**
PLMOF(Co)	**S/CNT**	**0.2**	**1392**	**100**	**878**	***This work***
		0.5	**1325**	**100**	**956**	
		0.5	**1325**	**200**	**846**	
		1	**1043**	**300**	**720**	
		2	**832**	**300**	**643**	

Table S2. A comparison of interlayer loading amount in this work with previously reported studies.

Interlayer Materials	Areal density of interlayer (mg cm^{-2})	C Rate	1st Capacity (mAh g^{-1})	Cycle	Capacity retention (mAh g^{-1})	Ref.
Y-FTZB	1.2	0.25	987	100	~650	[2] ACS Energy Lett.
B/2D MOF-Co	0.37	0.5	801	100	795	[4] Adv. Mater.
CNT@ZIF-30	0.9	0.2	1588	100	870	[5] Energy Stor. Mater.
VN	1.52	0.5	1050	100	860	[9] ACS Appl. Mater. Inter.
Cr_3C_2	0.75	0.5	865	100	~795	[10] Ind. Eng. Chem. Res.
Co_3Mo_3C	0.5	0.1	1251	100	905	[11] Sci. China Mater.
Ni-Co-P@C	0.4	0.5	1000	100	~700	[12] Energy Stor. Mater.
MWCNT/NCQD	0.15	0.5	~1120	100	~860	[14] Adv. Energy Mater.
UiO-66-S	1.1	0.2	1127	100	~1010	[15] J. Mater. Chem. A
Ti_3C_2Tx/S-A	0.7	0.1	1072	100	807	[16] J. Alloys Compd.
CNTs@CP/rGo	0.28	0.5	-	100	~800	[17] ACS Appl. Energy Mater.

PLMOF(Co)	**0.32**	**0.5**	**1325**	**100**	**956**	***This work***
	0.16		**1321**		**854**	
	0.08		**1215**		**705**	

Reference

[1] C. Chen, Q. Jiang, H. Xu, Z. Lin, Highly efficient synthesis of a moisture-stable nitrogen-abundant metal-organic framework (MOF) for large-scale CO_2 capture, Ind. Eng. Chem. Res., 58 (2019) 1773-1777.

[2] M. Li, Y. Wan, J. K. Huang, A.H. Assen, C. E. Hsiung, H. Jiang, Y. Han, M. Eddaoudi, Z. Lai, J. Ming, Metal-organic framework-based separators for enhancing Li-S battery stability: mechanism of mitigating polysulfide diffusion, ACS Energy Lett., 2 (2017) 2362-2367.

[3] Y. Zang, F. Pei, J. Huang, Z. Fu, G. Xu, X. Fang, Large-area preparation of crack-free crystalline microporous conductive membrane to upgrade high energy lithium-sulfur batteries, Adv. Energy Mater., 8 (2018) 1802052.

[4] Y. Li, S. Lin, D. Wang, T. Gao, J. Song, P. Zhou, Z. Xu, Z. Yang, N. Xiao, S. Guo, Single atom array mimic on ultrathin MOF nanosheets boosts the safety and life of lithium-sulfur batteries, Adv. Mater., 32 (2020) 1906722.

[5] F. Wu, S. Zhao, L. Chen, Y. Lu, Y. Su, Y. Jia, L. Bao, J. Wang, S. Chen, R. Chen, Metal-organic frameworks composites threaded on the CNT knitted separator for suppressing the shuttle effect of lithium sulfur batteries, Energy Stor. Mater., 14 (2018) 383-391.

[6] Y. Guo, M. Sun, H. Liang, W. Ying, X. Zeng, Y. Ying, S. Zhou, C. Liang, Z. Lin, X.

Peng, Blocking polysulfides and facilitating lithium-ion transport: polystyrene sulfonate@HKUST-1 membrane for lithium-sulfur batteries, ACS Appl. Mater. Inter., 10 (2018) 30451-30459.

[7] H. Chen, Y. Xiao, C. Chen, J. Yang, C. Gao, Y. Chen, J. Wu, Y. Shen, W. Zhang, S. Li, Conductive MOF-modified separator for mitigating the shuttle effect of lithium-sulfur battery through a filtration method, ACS Appl. Mater. Inter., 11 (2019) 11459-11465.

[8] S. Suriyakumar, A.M. Stephan, N. Angulakshmi, M.H. Hassan, M.H. Alkordi, Metal-organic framework@SiO_2 as permselective separator for lithium-sulfur batteries, J. Mater. Chem. A, 6 (2018) 14623-14632.

[9] Y. Song, S. Zhao, Y. Chen, J. Cai, J. Li, Q. Yang, J. Sun, Z. Liu, Enhanced sulfur redox and polysulfide regulation via porous VN-modified separator for Li-S batteries, ACS Appl. Mater. Inter., 11 (2019) 5687-5694.

[10] X. Liu, G. Feng, Y. Li, C. Xu, Q. Pan, Z. Wu, B. Zhong, X. Guo, S. Zhang, X. Xu, Novel interlayer on the separator with the Cr_3C_2 compound as a robust polysulfide anchor for lithium-sulfur batteries, Ind. Eng. Chem. Res., 59 (2020) 7538-7545.

[11] Z. Zhang, J. N. Wang, A. Shao, D. G. Xiong, J. W. Liu, C. Y. Lao, K. Xi, S. Y. Lu, Q. Jiang, J. Yu, Recyclable cobalt-molybdenum bimetallic carbide modified separator boosts the polysulfide adsorption-catalysis of lithium sulfur battery, Sci. China Mater., 63 (2020) 2443-2455.

[12] Z. Wu, S. Chen, L. Wang, Q. Deng, Z. Zeng, J. Wang, S. Deng, Implanting nickel and cobalt phosphide into well-defined carbon nanocages: A synergistic adsorption-electrocatalysis separator mediator for durable high-power Li-S batteries, Energy Stor.

Mater., 38 (2021) 381-388.

[13] X. Xiang, J.Y. Wu, Q.X. Shi, Q. Xia, Z.G. Xue, X.L. Xie, Y.S. Ye, Mesoporous silica nanoplates facilitating fast Li^+ diffusion as effective polysulfide-trapping materials for lithium-sulfur batteries, J. Mater. Chem. A, 7 (2019) 9110-9119.

[14] Y. Pang, J. Wei, Y. Wang, Y. Xia, Synergetic protective effect of the ultralight MWCNTs/NCQDs modified separator for highly stable lithium-sulfur batteries, Adv. Energy Mater., 8 (2018) 1702288.

[15] J. Han, S. Gao, R. Wang, K. Wang, M. Jiang, J. Yan, Q. Jin, K. Jiang, Investigation of the mechanism of metal-organic frameworks preventing polysulfide shuttling from the perspective of composition and structure, J. Mater. Chem. A, 8 (2020) 6661-6669.

[16] Q. Meng, Q. Jin, X. Wang, W. Lv, X. Ma, L. Li, L. Wu, H. Gao, C. Zhu, X. Zhang, 3D Ti_3C_2Tx aerogel-modified separators for high-performance Li-S batteries, J. Alloys Compd., 816 (2020) 153155.

[17] Z. Li, S. Jiao, D. Yu, Q. Zhang, K. Liu, J. Han, Z. Guo, J. Liu, L. Wang, Cationic-polymer-functionalized separator as a high-efficiency polysulfide shuttle barrier for long-life Li-S battery, ACS Appl. Energy Mater., 4 (2021) 2914-2921.